



Experimental Analysis and Finite Element Modeling of S-Core Sandwich Panel Composites Drop Impact Response

Hasan Murat ÖZTEMİZ^{1*}, Şemsettin TEMİZ²

¹ Kahramanmaraş İstiklal University, Elbistan Vocational School, hmoztemiz@gmail.com, Orcid No: 0000-0002-3609-3777

² Inonu University, Mechanical Engineering Department, semsettin.temiz@inonu.edu.tr, Orcid No 0000-0002-6737-3720

ARTICLE INFO

Article history:

Received 25 September 2023
Received in revised form 3 January 2024
Accepted 15 January 2024
Available online 29 March 2024

Keywords:

Low-velocity drop impact test,
Sandwich panel composites,
Mechanical behavior, S-core, Finite
element modeling

ABSTRACT

Sandwich panel composites have several applications in material technology. The sandwich panel composite material is constructed of stainless steel-316 for the top and bottom plates, aluminum 1050A-0 for the core, and DP-8405 acrylic adhesive for the binding element. The impact behavior of S-core composite sandwich panels was examined using low-velocity drop impact tests and finite element models. Finite element models have been created to characterize the influence of composite element bending behavior on variations. The specific flexural modulus and strength of composite S-core sandwich structures are equivalent to those found in the literature for core structures. As a result, the minimum weight design served as a guideline for producing weight and density-efficient hybrid composite sandwich panels. The energy absorbed in the test findings rose between 15.15% and 30% as the core thickness grew and between 3.571% and 41.34% as the core arrays changed. Impact load-bearing capability increases with varied core heights and array designs.

Doi: 10.24012/dumf.1365978

* Corresponding author

Introduction

Lightness, high strength [1], high fatigue resistance [2], and form retention, structural and impact strength [3-6], high bending stiffness, strength, and energy absorption capacity are all characteristics of composite materials that are employed in engineering applications such as aircraft, transportation, construction, electronics, and the food industry. It is chosen over traditional materials in applications requiring high wear, corrosion resistance, resistance to dynamic impact events, low density, and flexibility to achieve complicated forms [7-9]. Sandwich composites, for example, are favoured in airplane interiors such as floor panels, internal walls, food preparation rooms, and passenger storage racks [10]. In the broad preference for sandwich composite panels, increasing the material and geometric arrangement in the core structure, compression qualities (bending and buckling resistance), shear stiffness, high energy absorption ability [8-11], and lightness are very beneficial. The majority of these components (sandwich panels) are made up of surface materials as well as honeycomb and foam core materials [11-13]. Sandwich composite panels with open-cell core materials, in particular, give multifunctional benefits to the composite material, such as high stiffness and specific

strength [14-15]. Sandwich structure mechanical behavior, performance, and failure mechanisms (compression, shear or indentation failures, separation, and crushing) are determined by the material characteristics and geometry of their respective components (surface plates and core topology design) [6], [9]. With component geometry, high-performance sandwich composite panels may be created [16-18]. Surface materials in sandwich composite panels should be composed of hard components in the sandwich, be resistant to shear and bending loads [19], and be resistant [20] to plane separation [21]. Honeycomb sandwich structures are made up of a substantial core material sandwiched between two thin layers of hard surface material. While the honeycomb core material keeps the sandwich panel's stiffness and energy absorption capabilities, its hollow cellular structure provides lightness to the sandwich panel. In applications requiring high strength, such as automotive and aerospace, honeycomb sandwich composite panels are commonly employed instead of conventional materials [21-23]. A honeycomb profile [24] and chain, pyramid grooved [25], x-type, kagome-type, hybrid, and unique designs [26-28] can be used as the core structural geometry. The energy absorption and damage load performances of composite materials were evaluated and optimized using falling

weight impact tests on different core arrays and core profiles [29-31] to establish the most appropriate design. Changes to the core geometry result in enhancements to the damage mechanisms [32]. The links between damaged formations and changes in core and matrix deformations that occur under various energy loads on the composite material are investigated, and optimal design parameters are identified [33]. The falling weight impact tests of different core array variations of a sandwich composite panel with a unique core design, S-shaped 1050-O series aluminum core structure, 316 stainless steel upper and lower layers, and DP-8405 acrylic adhesive as binding element were investigated experimentally and numerically in this study. They were compared to finite element analysis analyses performed using the package software, and their mechanical behavior was studied.

2. Experimental Method

The surface layer in this investigation was 1 mm thickness, and 170x100 mm dimensions stainless steel-316, while the core material was aluminum 1050A-0 alloy. The bonding ingredient between the bottom-upper plate and the core was DP-8405 acrylic glue. Table 1 shows the physical and mechanical parameters of aluminum 1050A-0 and stainless steel-316.

Table 1. Mechanical properties of Aluminum 1050A-0 and Stainless steel-316 alloys [34-36]

	Aluminum 1050A-0	316-Stainless Steel
Density	2710 kg/m ³	7800 kg/m ³
Tensile Yield Strength	37,94 MPa	200 MPa
Tensile Ultimate Strength	80 MPa	515 MPa
Modulus of Elasticity	69 GPa	200 GPa
Elongation (%)	40	40
Shear Modulus	50 MPa	82 GPa
Poisson Ratio	0,33	0,275

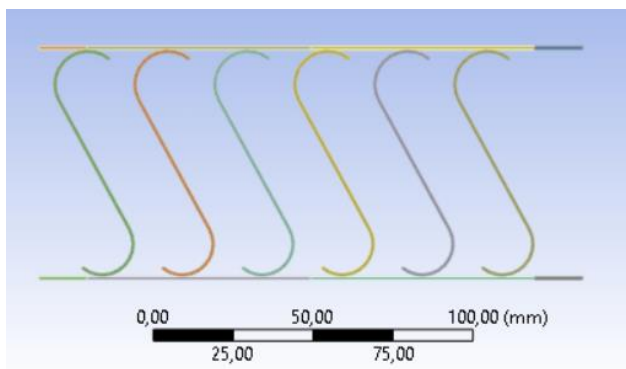


Figure 1. S-core sandwich panel composite drawing view S-core sandwich panel composite with a core height of 70 mm, and thickness of 0.7 mm drawing specimen view is given in Figure 1.

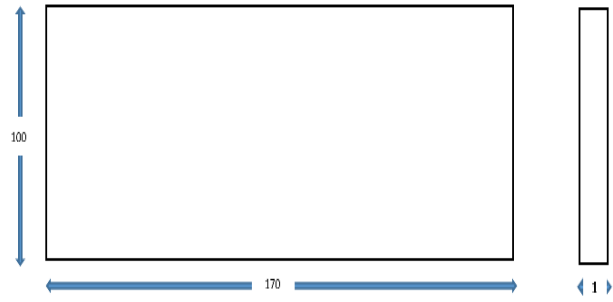


Figure 2. Bottom and top sheet dimensions

The dimensions of the lower and upper plates made of 1mm thickness, and 170x100mm dimensions stainless steel-316 material are given in Figure 2.

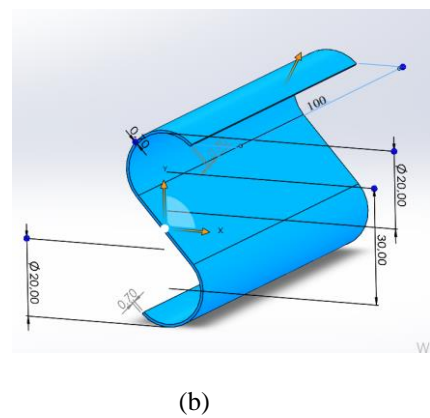
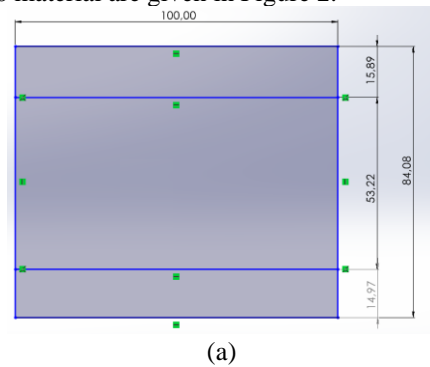
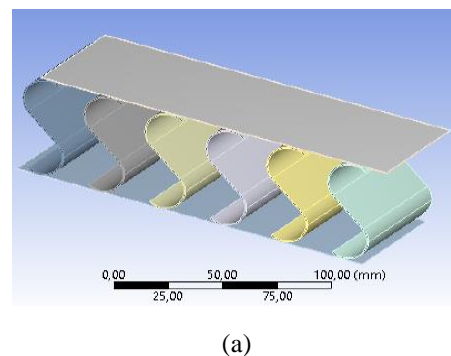
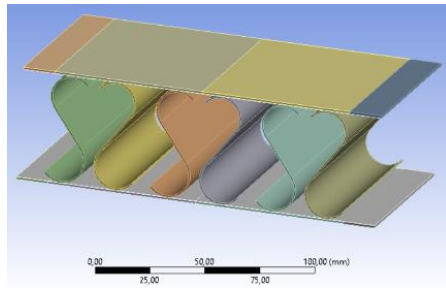
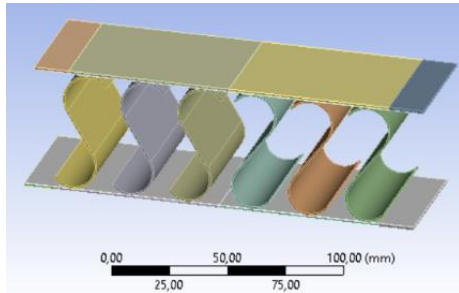


Figure 3. S-core selected for R10mm; a) before bending, b) bending dimensions, c) post bending view The S-core R10mm dimensions of the core structure to be produced with different wall thicknesses and the sheet dimensions before and after bending are given in Figure 3.

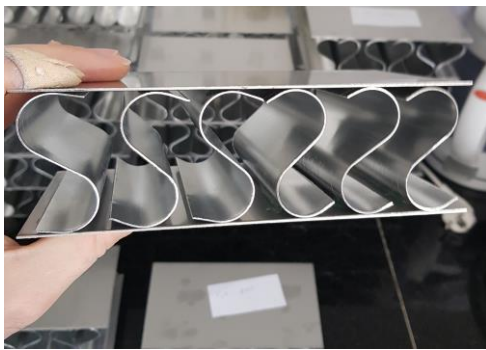




(b)



(c)



(d)

Figure 4. S-core aluminum sandwich composite panel; (a) straight row drawing view [37], (b) one straight one reverse row drawing view, (c) three straight three reverse rows drawing view [38], (d) three straight three reverse rows test specimens

Composite panel working groups are shown in Figure 4. Fig 4b, and 4c 3D views are about bending behavior of S-core sandwich panel and this paper used to same specimens dimensions data. The dimension of distance between the cores of all samples was taken as 25 mm.

Table 2. Dimensions of S-Core Sandwich Aluminum Composite Sheet Variations (Core Arrays: Straight:S, Straight-Reverse:S-R, Three Straight- Three Reverse: 3S-3R)

Core Array	Group code	Core wall thickness t, (mm)	Core Height (mm)	Core radius (mm)	Weight (gr)	Density (kg/m ³)
S	S1	0.6	50	R7.5	12.40	14.0271
	S2	0.7	50	R7.5	12.60	14.2534
	S3	0.8	50	R7.5	13.35	15.1018
	S4	0.6	50	R10	13.10	14.8190
	S5	0.7	50	R10	13.35	15.1018
	S6	0.8	50	R10	14.30	16.1764
	S7	0.6	50	R12.5	13.45	15.2149
	S8	0.7	50	R12.5	13.60	15.3846
	S9	0.8	50	R12.5	14.85	16.7986
	S10	0.7	60	R10	13.60	12.9032
S-R	S12	0.7	70	R10	14.70	12.0098
3S-3R	S13	0.7	50	R10	13.35	15.1018

Table 2 shows the dimensions of the S-core sandwich aluminum composite sheet variants. In this work, testing and analyses were done for samples with distinct core sequences in meridian wall thickness values, in addition to variable core wall thickness and radius values.

2.1. Dynamic drop test

A drop-weight impact test is performed by dropping a given weight from a predetermined height on the sample. Drop-weight tests are classified as either with or without instrumentation. The instrumented drop-weight impact test method is used to evaluate the dynamic properties of the material. Unlike earlier techniques, using different weights and changing different heights may provide the necessary energy, and the impact test system can perform the sticking, piercing, and repeated impact tests on the sample [37-38]. ACI 544.2R-89 [39] instrumented and conducted drop-weight impact tests on an Instron Ceast 9350 testing machine.



(a)

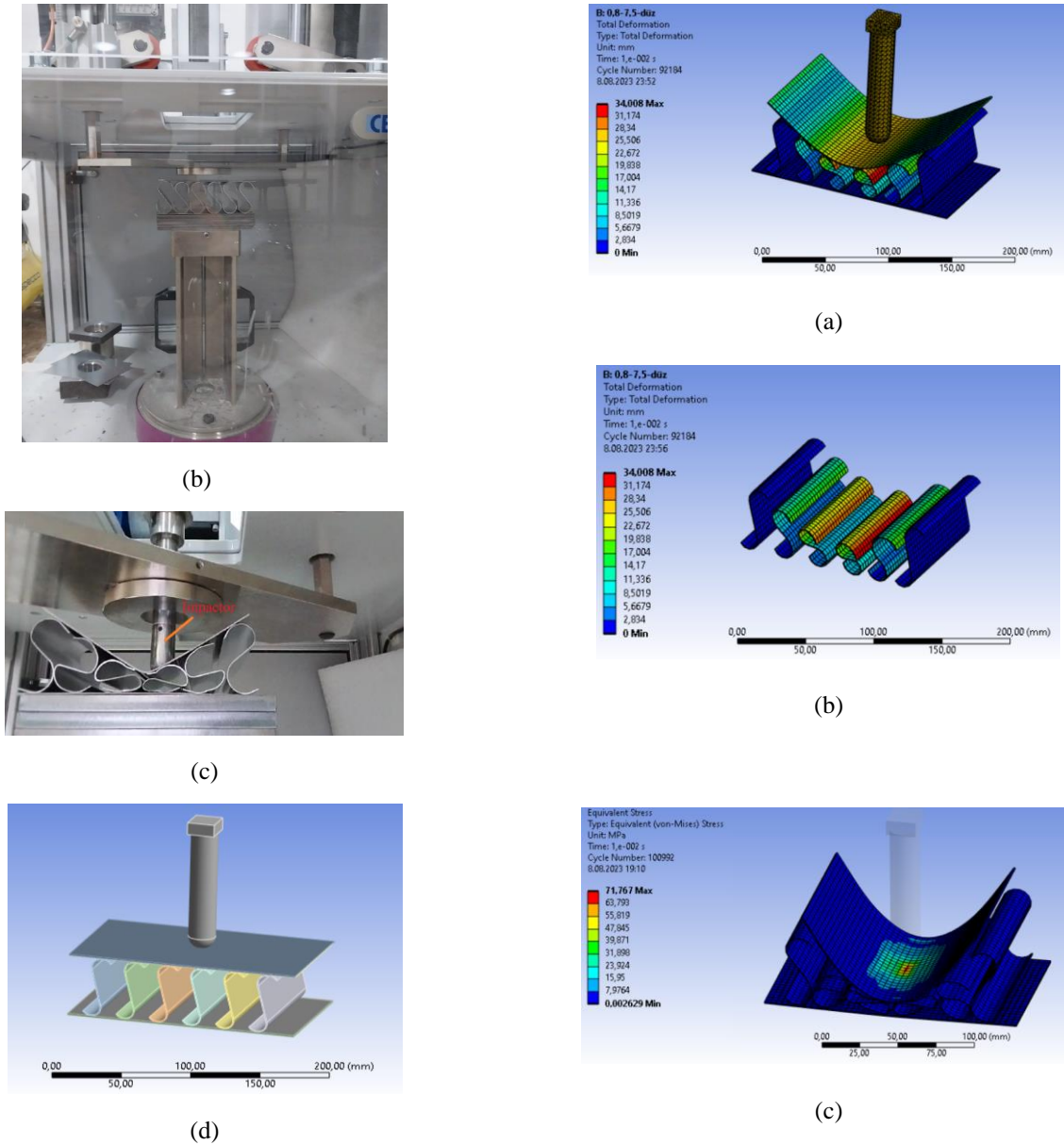


Figure 5. Instrumented drop-weight test machine. (a) Instron 9350, (b) Test setup for the composite plate, (c) Test finished for composite plate, (d) ANSYS drop-weight analysis model

Since the bottom and top layers of the composite panel have a yield strength of more than five times that of the core material, the optimum working energy value, determined by the preliminary study carried out in the Ansys software and finite element analysis data, was determined as 40 Joule. The drop-weight test apparatus is depicted in full in Figure 5. The energy of impact was 40 Joule. In each research group, the exam was repeated four times.

3. Results and Discussions

The following study results were gathered as a consequence of the drop-weight impact analysis and experimental application.

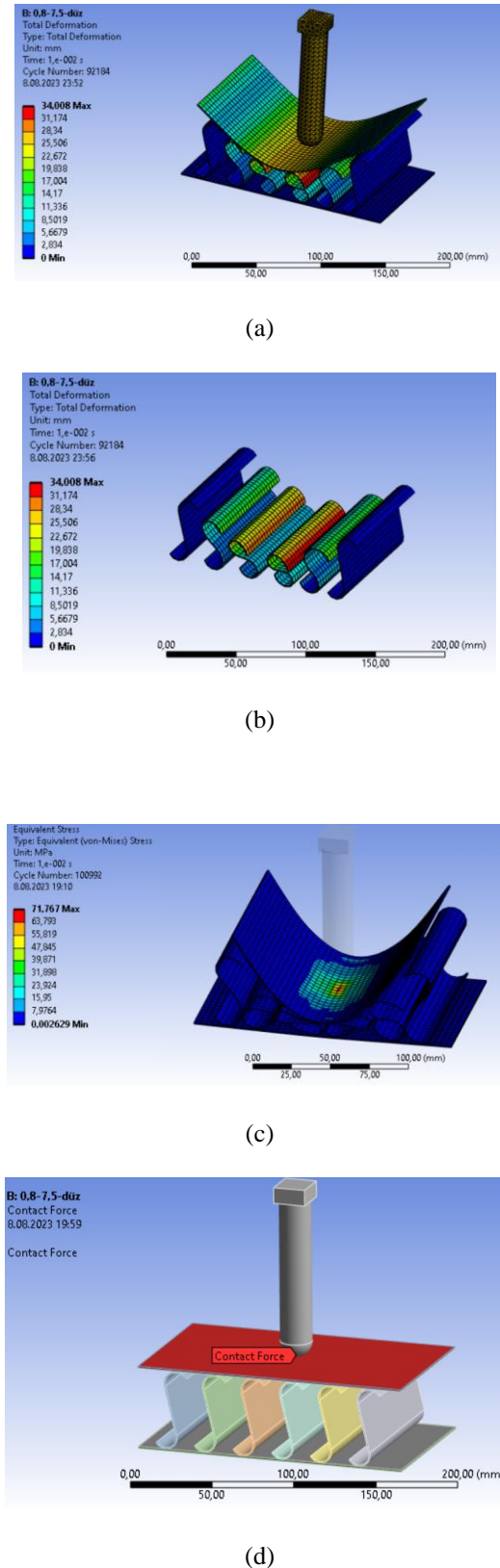
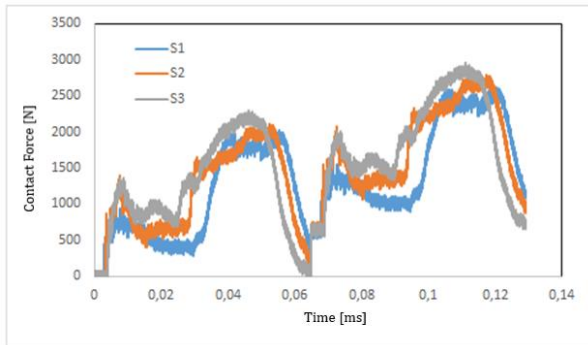


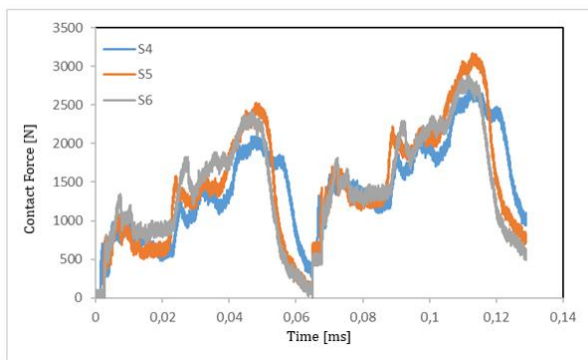
Figure 6 Total deformation a) Specimen S12, b) Specimen S3 cores, and c) Specimen S12 Equivalent stress, d) Specimen S3 contact force

The falling weight in the drop-weight impact test is 10.5 kg, and the analysis and testing were performed with 40 J energy obtained from a height of 0.388 m, the ambient

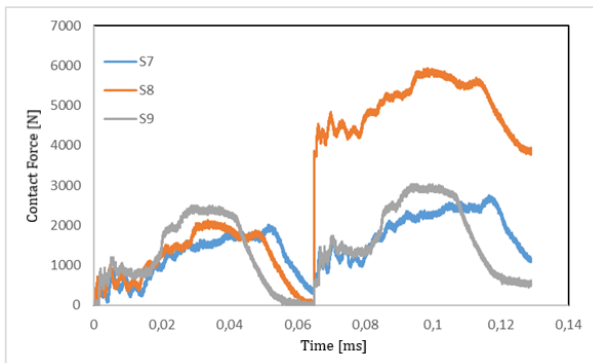
temperature was 23.8 °C, and the relative humidity was 46%. The test operations were repeated four times, and the average data were collected.



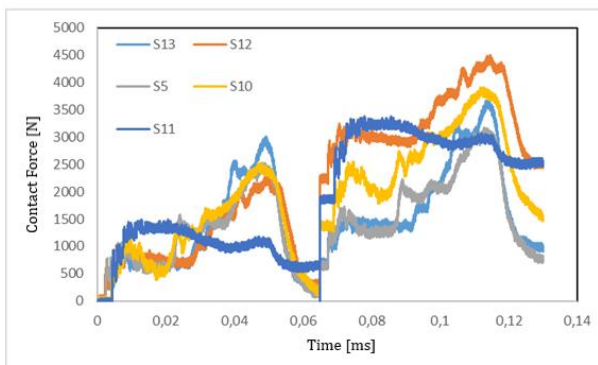
(a)



(b)



(c)



(d)

Figure 7 Specimens contact force- time graphs a) S1, S2, and S3 b) S4, S5, and S6 c) S7, S8, and S9 d) S5, S10, S11, S12, and S13

As seen in Figs. 7a-b-c, the contact force increased as the material wall thickness decreased. Figure 7-d depicts the change in impact force with varied core arrays and core height. While S5 and S10 reacted similarly, the alteration in the core sequence in S12 had the greatest impact value.

Table 3 shows the contact force data for the many variants in which the falling weight impact test and analysis procedure were used, as well as the proportional differences between these data.

Table 3. Contact force data for samples subjected to drop weight impact testing and analysis.

Specimens	Test	Analysis	% Difference
S1	1941.39	1625.7	-0.19419
S2	1398.65	1421.3	0.016207
S3	1363.598	1370.6	0.005109
S4	1490.71	1557.8	0.043067
S5	1548.49	13192	-0.17381
S6	1340.486	1195,6	-0.12118
S7	1560.048	1355,5	-0.1509
S8	1444.48	1355,5	-0.06564
S9	1190.26	1215,9	0.021087
S10	2472.96	2102,1	-0.17642
S11	1935.615	2105,1	0.080512
S12	2288.07	2203,8	-0.03824
S13	2530.74	2109,3	-0.1998

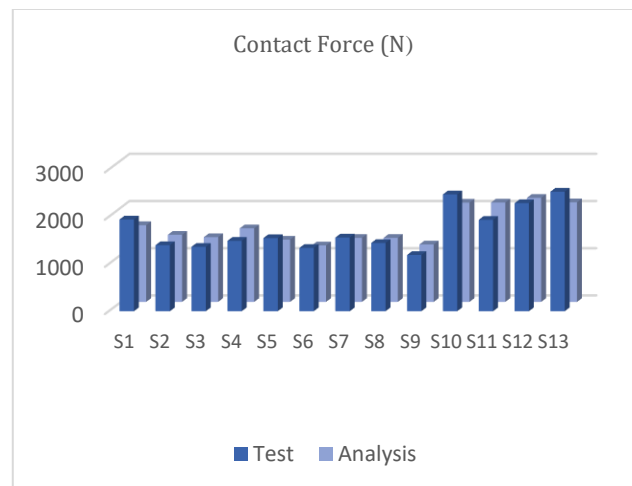
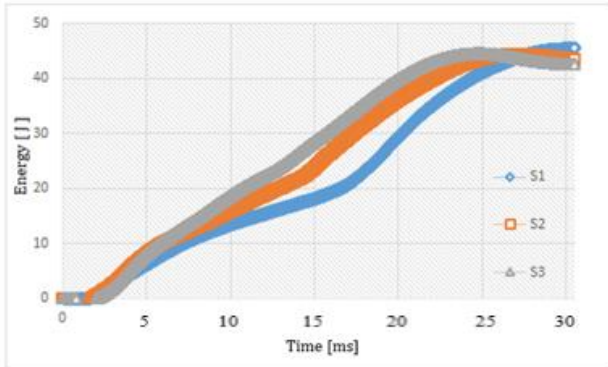


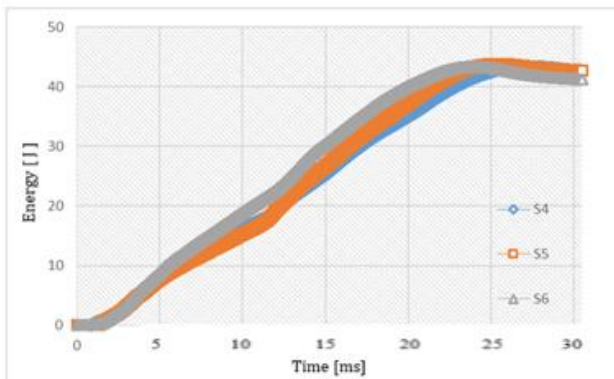
Figure 8. Contact force histogram of the studied variations

In the impact analysis and test data, damage was first observed in the core material group. The determination of the damage load formation time and the contact force as a result of the impact effect in the working groups was made

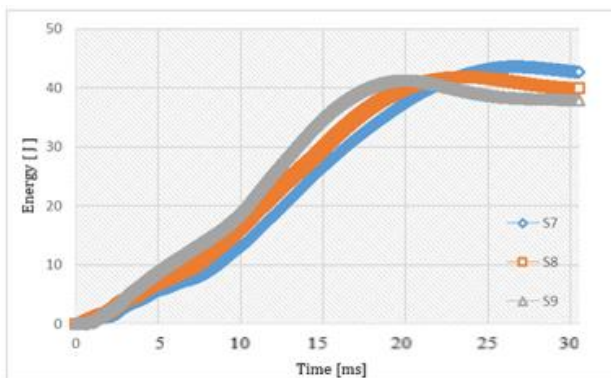
with the damage time data. Proportional differences between the study groups vary between 0.5109 and 19%. In general, the test and analysis results are compatible with each other.



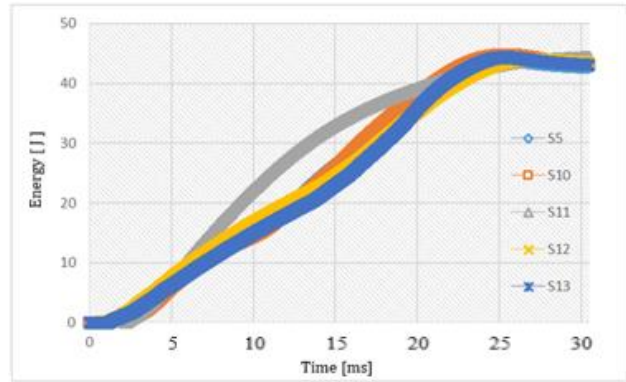
(a)



(b)



(c)



(d)

Figure 9. Energy time graph formed by impact test, a) S1, S2, and S3 specimens, b) S4, S5, and S6 specimens, c) S7, S8, and S9 specimens, d) S5, S10, S11, S12, and S13 specimens

As can be seen in Figure 9 a, b, and c, increasing the core wall thickness increases the energy dissipation ability. In Figure 9a, the energy dissipation of variation S3 occurred 20.1% earlier than variation S1. Figure 9d, The shortest energy dissipation ability occurred in S11, and the longest dissipation was achieved in variation S12. There is a time delay of 13.04% between these two variations. For the operating energy scale (40J), the difference in core alignment provided more efficiency than the changes in core wall thickness and core radius parameters.

4. Conclusions

When the numerical stress analysis and test results of the S-shaped sandwich panel exposed to the falling weight impact test with varied core radii, height, and wall thicknesses were analyzed, the following findings were obtained.

- When the impact loads were studied, it was discovered that as the core thicknesses grew, so did the impact loads. This is due to the fact that as the thickness of the core materials grows, so does the moment of inertia.
- The impact load-carrying ability increased when the core sequence of the examined samples was changed. (The impact load-bearing capability of the S12 sample is 47.76% more than that of the S5.)
- The energy dissipation ability was realized in close periods with each other in all research samples, with the S9 sample having the quickest damping time due to the variation in the core wall thickness.
- The impact load capacity of the S10 and S11 samples, which were generated by a change in core height compared to the S5 sample, has increased to values ranging from 59.7 to 25% due to their high moment of inertia.

The S-shaped core structure, conceived and assessed as a new core form, will contribute to the literature by utilizing

various material selections, fillers, and binding components. Its goal is to investigate the novel forms specified in future investigations.

Acknowledgment

This research was supported by Inonu University (BAP Project Code: FDK-2020-2306). The authors thank Inonu University for funding the project.

Contributions of the authors

Corresponding author contributions this paper

-Working concept and design

-Data collecting

-Analysis and interpretation of data

Second author contributions this paper

-Revision

Conflict of Interest Statement

There is no conflict of interest between the authors.

Statement of Research and Publication Ethics

The study is complied with research and publication ethics.

References

- [1] M.Ş. Adin, E. Kılıçkap, "Strength of double-reinforced adhesive joints," *Materials Testing*, Feb 23, 2021. DOI: [10.1515/mt-2020-0024](https://doi.org/10.1515/mt-2020-0024)
- [2] H. Adin , B. Yıldız, M.Ş. Adin , "NUMERICAL INVESTIGATION OF FATIGUE BEHAVIOURS OF NON-PATCHED AND PATCHED ALUMINIUM PIPES, " *European Journal of Technique (EJT)*, Volume: 11 Issue: 1, 60 – 65, 2021, DOI: [10.36222/ejt.893327](https://doi.org/10.36222/ejt.893327)
- [3] M. Arslan , O. Güler, U. Alver, " The investigation of the mechanical properties of sandwich panel composites with different surface and core materials". *Pamukkale University Journal of Engineering Sciences*, 24(6),1062-1068, 2018
- [4] S. Chen, X. Tan, J. Hu, S. Zhu, B. Wang, L. Wang, Y. Jin, L. Wu, "A novel gradient negative stiffness honeycomb for recoverable energy absorption," *Composites Part B: Engineering* ,Volume 2, 108745, 2021
- [5] J. Cao, K. Cai, Q. Wang, J. Shi, "Damage behavior of a bonded sandwich beam with corrugated core under 3-point bending, *Material Design* Volume, " 95, 165-172, 2016
- [6] Y.Zhang, T. Liu, W. Tizani, "Experimental and numerical analysis of dynamic compressive response of Nomex honeycombs," *Composite Part B:Engineering*, Volume 148, 27-39, 2018
- [7] X. Wu , H. Yu, L. Guo, L. Zhang, X. Sun, Z. Chai, "Experimental and numerical investigation of static and fatigue behaviors of composites honeycomb sandwich structure," *Composite Structure*, 165-172, 2019
- [8] G. Xu, F. Yang, T. Zeng, S. Cheng, Z. Wang, "Bending behavior of graded corrugated truss core composite sandwich beams," *Composite Structure*, 342-251, 2016
- [9] T. Li, L. Wang, "Bending behavior of sandwich composite structures with tunable 3D-printed core materials," *Composite Structure*, 46-57, 2017
- [10] F.C. Potes, J.M. Silva, P.V. Gamboa, "Development and characterization of a natural lightweight composite solution for aircraft structural applications," *Composite Structures*, 430-440, 2016
- [11] J. Forsberg, L. Nilsson, "Evaluation of response surface methodologies used in crashworthiness optimization," *International Journal of Impact Engineering*, 759-777, 2006
- [12] G. Qi, Y.L. Chen, P. Richert , L. Ma , K.U. Schröder, "A hybrid joining insert for sandwich panels with pyramidal lattice truss cores," *Composite Structures*, 241, 112-123, 2020
- [13] X. Lu, V.B.C Tan, T.E. Tay, "Auxeticity of monoclinic tetrachiral honeycombs," *Composite Structures*, Volume 241, 112067
- [14] K. Naresh, W.J. Cantwell, "Single and multi-layer core designs for Pseudo-Ductile failure in honeycomb sandwich structures," *Composite Structures*, Volume 256, 113059, 2021
- [15] S. Newstead, L. Watson, M. Cameron., "Vehicle Safety Ratings Estimated From Police Reported Crash Data: 2008 Update," *Monash University Accident Research Center Report*, Melbourne, Australia, 280, 2008
- [16] X.M. Xiang, G. Lu., Z.H. Wang, "Quasi-static bending behavior of sandwich beams with thin-walled tubes as core," *Int J Mech Sci*, 55-62, 2015
- [17] A. Petras, M.P.F. Sutcliffe, "Failure mode maps for honeycomb sandwich panels," *Composite Structure*, 237-252, 1999

- [18] Z. Sun, S. Shi, X. Hu, X. Guo, J. Chen, "Short-aramid-fiber toughening of epoxy adhesive joint between carbon fiber composites and metal substrates with different surface morphology," *Composite Part B Engineering*, 38-45, 2015
- [19] H. Adin, M.Ş. Adin, "Effect of particles on tensile and bending properties of jute epoxy composites," *Materials Testing*, March 16, 2022. DOI: [10.1515/mt-2021-2038](https://doi.org/10.1515/mt-2021-2038)
- [20] H.B. Rachid, D. Nouredine, B. Benali, M.Ş. Adin, M.Ş., "Effect of nanocomposites rate on the crack propagation in the adhesive of single lap joint subjected to tension," *MECHANICS OF ADVANCED MATERIALS AND STRUCTURES*; JUL 22 2023, DOI: [10.1080/15376494.2023.2240319](https://doi.org/10.1080/15376494.2023.2240319)
- [21] S.D. Pan, L.Z. Wu, Y.G. Sun, Z.G. Zhaou, "Fracture test for double cantilever beam of honeycomb sandwich panels," *Materials Letters*, 62, 523-526, 2008
- [22] Q. Qin, S. Chen, K. Li, M. Jiang, T. Cui, J. Zhang, "Structural impact damage of metal honeycomb sandwich plates," *composite*, Volume 252, 112719, 2020
- [23] Q.H. Qin, T.J. Wang, "Low-velocity impact response of fully clamped metal foam core sandwich beam incorporating local denting effect," *Composite Structures*, Volume 96, 346-356, 2013
- [24] X. Zhang, F. Xu, Y. Zang, W. Feng, "Experimental and numerical investigation on damage behavior of honeycomb sandwich panel subjected to low-velocity impact," *composite structure*, Volume 236, 111882, 2020
- [25] J. Xiong, L. Ma, L. Wu, B. Wang, and A. Vaziri, "Fabrication and crushing behavior of low-density carbon fiber composite pyramidal truss structures," *Composite Structures*, Volume 92, 2695-2702, 2010
- [26] H.P. Wang, C.T. Wu, Y. Guo, E. Mark, A. Botkin, "Coupled meshfree/finite element method for automotive crashworthiness simulations," *International Journal of Impact Engineering*, 36(10-11), 1210-1222
- [27] J. Mei, J. Liu, W. Huang, "Three-point bending behaviors of the foam-filled CFRP X-core sandwich panel: Experimental investigation and analytical modelling," *Composite Structures*, Volume 284, 11520, 2022
- [28] V.S. Sokolinsky, H. Shen, "Vaikhanski L and Nutt SR., Experimental and analytical study of nonlinear bending response of sandwich beams," *Composite Structures*, 60, 219-229, 2003
- [29] A. Boukar, S. Corn, P. Slangen, P. Ieny, "Finite element modelling of low velocity impact test applied to biaxial glass fiber reinforced laminate composites," *International Journal of Impact Engineering* 165, 104218, 2022
- [30] G. Belingardi, R. Vadori, "Low velocity impact tests of laminate glass-fiber-epoxy matrix composite material plates," *International Journal of Impact Engineering* 27, 213-229, 2002
- [31] H. Yujia, M. Ming, Y. Siya, W. Kai, "Drop-weight impact behaviour of stitched composites: Influence of stitching pattern and stitching space," *Composites: Part A* 172, 107612, 2023
- [32] D. Lee, B. Park, S. Park, C. Choi, J. Song, "Fabrication of high-stiffness fiber-metal laminates and study of their behavior under low-velocity impact loadings," *Composite Structures*, 189, 61-69, 2018
- [33] H. Liu, Y. Zhou, L. Chen, X. Pan, S. Zhu, T. Liu, W. Li, "Drop-weight impact responses and energy absorption of lightweight glass fiber reinforced polypropylene composite hierarchical cylindrical structures," *Thin-Walled Structures* 184, 110468, 2023
- [34] Aluminum 1050-O. <https://www.matweb.com/search/DataSheet.aspx?MatGUID=273c1ffbdc134a8292c704da3ee2ff35>. Access date 18 August 2023
- [35] Stainless steel-Grade316. <https://www.azom.com/properties.aspx?ArticleID=863>. Access date 18 August 2023
- [36] Stainless steel 316. <https://www.matweb.com/search/DataSheet.aspx?MatGUID=3a413dabd215462da3408e6e8b761349>. Access date 18 August 2023
- [37] H.M. Öztemiz, Ş. Temiz, "Mechanical Behaviors Of Different Radii Of Curvature S-Shaped Core Sandwich Composites Subjected To Bending Load," *International Asian Congress On Contemporary Sciences-VI*, Van-Türkiye, 200-207, 27-29 May 2022
- [38] H.M. Öztemiz, Ş. Temiz, "Mechanical Behaviors Of Different Array With S-Shaped Core Sandwich Composites Subjected To Bending Load," *International Asian Congress On Contemporary Sciences-VI*, Van-Türkiye, 208-216, 27-29 May 2022

- [39] E.A. Alwesabi, B.H. Abu Bakar, I.M.H. Alshaikh, H.M. Akil, "Impact resistance of plain and rubberized concrete containing steel and polypropylene hybrid fiber," *Mater Today Commun*, DOI: 10.1016/j.mtcomm.2020.101640
- [40] M. Sahan M, I. Unsal, "An Experimental Analysis for Impact Behaviour of Portland Cement Concrete Substituted with Reclaimed Asphalt Pavement Aggregate, Iranian Journal of Science and Technology," *Transactions of Civil Engineering*, 47:2113–2130, 2023 DOI: 10.1007/s40996-023-01052-7
- [41] ACI 544.2R-89 (1999) Measurement of properties of fiber reinforced concrete. ACI Committee 544